MEMS gas sensor of resistive type for detection of hydrogen sulfide down to low concentrations

I.M. Komarevtsev [1] iD **, A.S. Kondrateva** [1] iD **, A.N. Kazakin** [1] iD **, Ya.B. Enns** [1] iD **,**

I.A. Lazdin [2✉] iD **, P.A. Karaseov** [2] iD **, U.D. Akulshin** [2] iD

[1] Alferov University, St. Petersburg, Russian Federation

[2] Peter the Great St. Petersburg Polytechnic University, St. Petersburg, Russian Federation

✉ bitbooks8@gmail.com

ABSTRACT
The technological route to manufacture a resistive-type MEMS gas sensor for low analyte concentration detection is proposed and the main characteristics of the device are demonstrated. MEMS consists of a silicon substrate with nickel interdigital electrodes acting as a microheater, on top of which a thin (100 nm) gas-sensitive layer of nickel oxide (NiO) is deposited. The silicon substrate is etched from the back side of the device to achieve a membrane of about 50 microns. The operating temperature of the sensitive layer in measurement mode is 130–205 °C. The proposed device shows the effect of introducing hydrogen sulfide in a gas mixture from 1 to 100 ppm on the conductivity of the sensing layer.
KEYWORDS
microelectromechanical system • nickel oxide • microelectromechanical resistive gas sensor • hydrogen sulfide

Introduction

Microelectromechanical systems (MEMS) are used in applications ranging from gyroscopes and accelerometers to air pollution detection systems [1–5]. At the same time, high-performance gas sensors with high sensitivity, selectivity, and low response time to small changes in gas concentration are still needed to improve reliability. Compact and MEMS sensors with low power consumption are one of the options for solving this problem.

The main difficulty in the application of MEMS as high-performance gas sensors of resistive type is the selection of the material of the gas-sensitive element, which can be thin films of metal oxides, metal-organic composites, nanocomposites and other materials [4–7]. The development of new topologies of microsystems and the search for the best materials for the sensitive layer is the actual task. At the same time, the choice of material for the sensitive layer of the gas sensor is based on the gas to be detected, thus, the study of sensitivity to different gases of different elements and compounds is also extremely important [8–10].

Hydrogen sulfide is a neurotoxic gas that causes poisoning if the content of the compound exceeds 50 ppm. The maximum permissible, or low, concentrations are less than 7 ppm for the work area and 0.008 ppm for the residential area. For measuring in the range of operating area concentrations of 1–1000 ppm, electrochemical sensors are used. They have low response rate, low resolution, and a bulky design, as well as low energy efficiency (only a few watts). Other methods of studying the concentration of gases in the mixture, such as mass spectrometry, chromatography and optical methods, are not suitable for conditions of continuous air quality monitoring, as they require special sample preparation and do not allow full automation of the process without the use of highly qualified personnel.

In turn among MEMS devices for detection of hydrogen sulfide the sensors based on tin oxide, tantalum oxide with various doping were used. It is shown that the presence of metal inclusions (zinc, copper, nickel, indium) increases the sensitivity and selectivity to this gas due to the formation of sulfides of these metals on the surface. The application of these sensors is limited by the long recovery time (it takes several hours for desorption) and/or degradation of the active layer [11]. The presence of oxidation centers on a sensitive layer is also important in detection of hydrogen sulfide. The presence of such centers is associated with both the crystallinity of a film, and the roughness of its surface.

One of the options for the material of the sensing element is nickel oxide. For films of nickel oxide, which acts as an active center for the addition of hydrogen sulfide, the possibility of achieving greater surface roughness was shown in the study of electrochromic properties [12]. In addition, the *p*-type conductivity of nickel oxide suggests a decrease in the conductivity of the material through the adsorption of hydrogen sulfide on its surface [13].

Thus, the purpose of this work was to create a MEMS gas sensor of resistive type with a thin-film sensing element of nickel oxide, suitable for detection in a gas mixture with a concentration of hydrogen sulfide from 1 to 100 ppm.

Methodology of manufacturing MEMS gas sensor

Functional diagram and design of the sensitive element

For manufacturing the laboratory prototype of the sensitive element (SE) of the MEMS hydrogen sulfide gas sensor, the classical functional scheme of resistive gas sensors [5] was chosen. It contains a heating element and a sensitive layer based on a semiconductor film that changes its conductivity by interaction with analyte molecules during adsorption and desorption of gas from the surface of the active layer [11].

The SE is made of monocrystalline silicon with a thickness of 0.4 mm and a size of 10 × 10 mm in the horizontal plane. In the central part, the silicon is thinned to a membrane with a thickness of about 50 μm to reduce power consumption and increase the SE performance (Fig. 1(b)). On the membrane, there are a heater and two interdigital electrodes separated by an insulating dielectric and made by thin-film technology from metal having an ohmic contact to the semiconductor layer of nickel oxide (Fig. 1(a)). For *p*-type NiO, nickel and gold, which have a high work function, can act as contacts. The heater is designed in the form of a meander, whose paths between the protrusions of the interdigital electrodes, and is covered with a protective dielectric from above, unlike the

protrusions of the electrodes [14]. The length of the protrusions of the interdigital electrodes is 2 mm, the distance between the protrusions is 300 μm, and the width of the heater track is 100 μm. The sensitive layer (NiO) is located on the membrane above all the elements and is in electrical contact only with the protrusions of the electrodes acting as a measuring element. With this configuration of the SE, the entire surface of the sensitive layer is open for interaction with the molecules of the analyzed gas, and the maximum heating is carried out directly between the protrusions of the measuring electrodes [15].
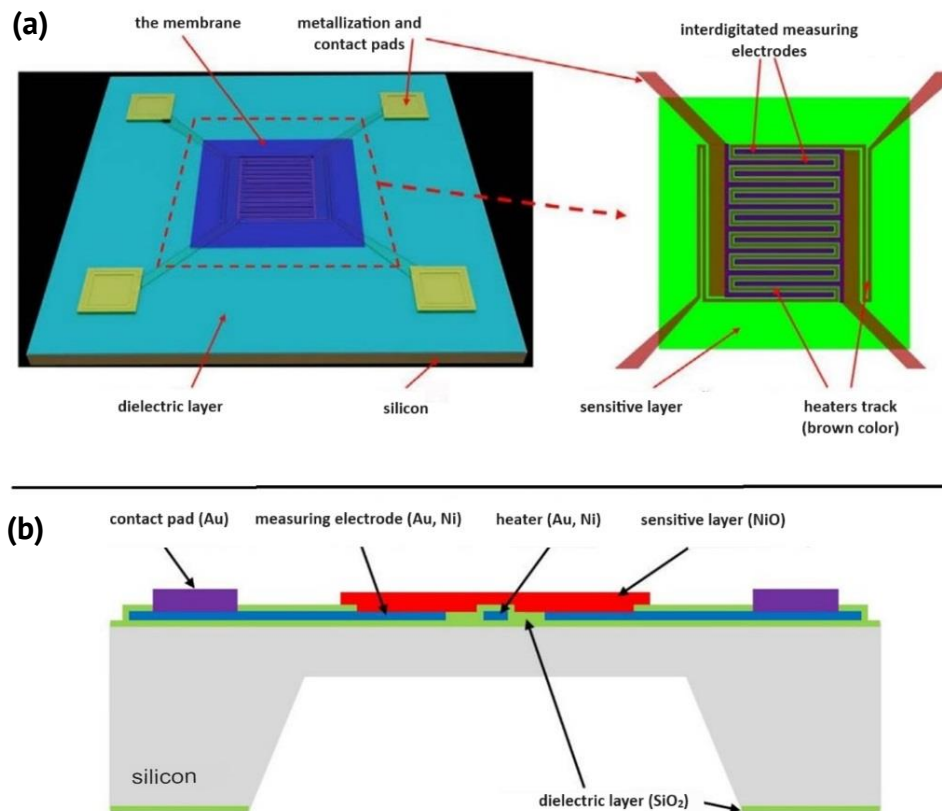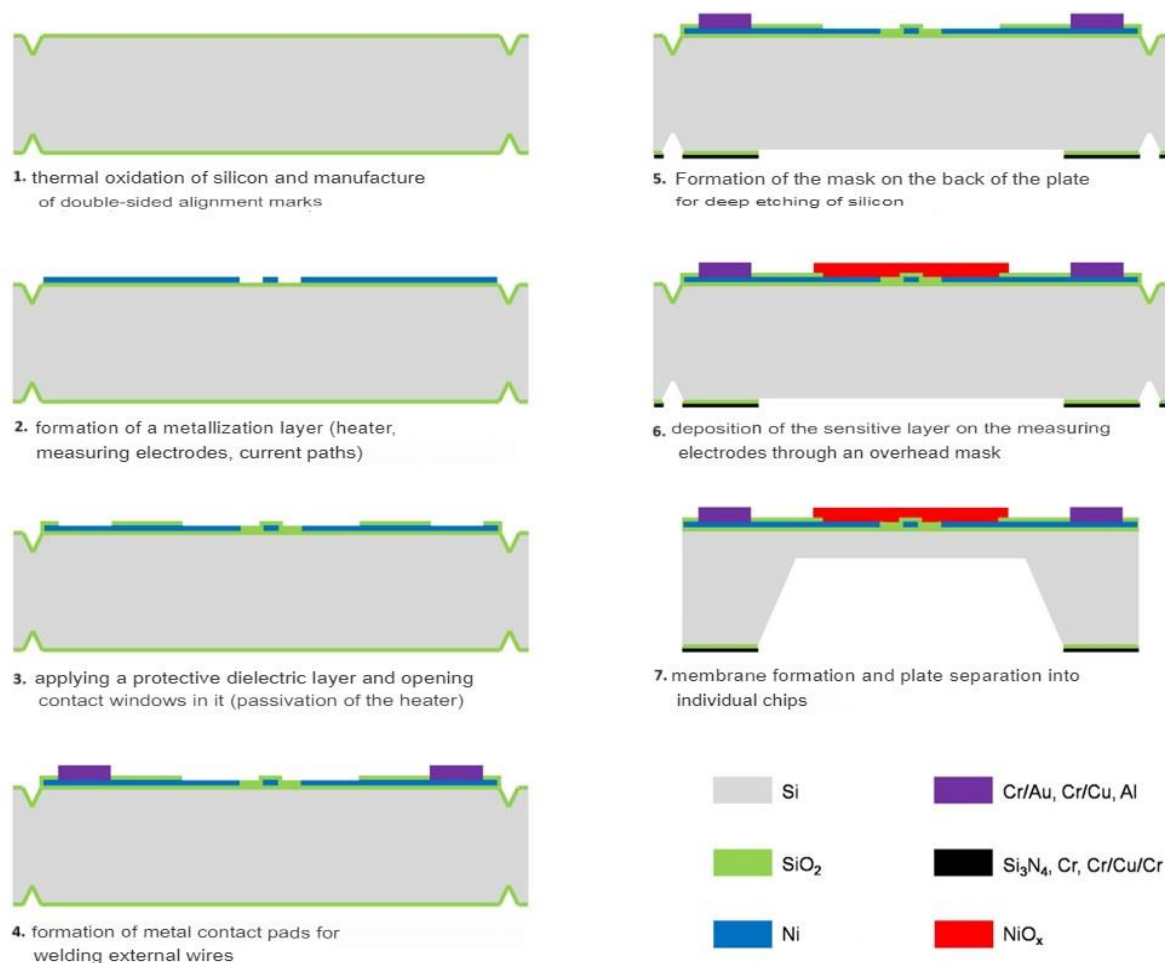

Fig. 1. Schematic diagram of the SE chip: (a) top view: chip size 10 × 10 × 0.4 mm; (b) side view (not to scale)

The performance, sensitivity, and selectivity of such a SE to the analyzed gas depend on the thickness and crystal structure of the NiO layer [15], regulated by the modes of its vacuum deposition and subsequent high-temperature annealing, as well as on the temperature mode of the SE operation, set by the heater [16,17].

The technological route presented in Fig. 2 was chosen for the fabrication of SE laboratory models. The presented route is universal, as it is suitable for the use of various gas-sensitive materials, such as nickel, titanium, molybdenum, tin oxides and others [8,9,18–20] with the use of metallization system based on noble metals and a plasma method of membrane formation. In addition, a nickel metallization system can be used to create an electrical contact to the gas-sensitive layer, and alkaline etching of silicon in potassium hydroxide solutions can be used to form a silicon membrane with low heat capacity.

Manufacturing MEMS hydrogen sulfide gas sensor

To precisely position the elements during the technological process, special marks were created on the plates for subsequent precise alignment of the elements located on the front (top) side of the plate and the back (bottom) side of the plate (Fig. 2). A ~ 100 nm thick SiO_2 oxide layer, grown by thermal oxidation for four hours at 950 °C, was coated with a positive photoresist, followed by double-sided photolithography. This was followed by etching the oxide in a standard SiO_2 buffer etchant for 1 min and 5 μm mark burial by wet etching of the silicon in 25 % tetramethylammonium hydroxide (TMAH) solution for 10 min at 70 °C. This was followed by cleaning aggregates from the surface and repeated thermal oxidation of the silicon for 4 h at 950 °C.

1. thermal oxidation of silicon and manufacture of double-sided alignment marks

2. formation of a metallization layer (heater, measuring electrodes, current paths)

3. applying a protective dielectric layer and opening contact windows in it (passivation of the heater)

4. formation of metal contact pads for welding external wires

5. Formation of the mask on the back of the plate for deep etching of silicon

6. deposition of the sensitive layer on the measuring electrodes through an overhead mask

7. membrane formation and plate separation into individual chips

Si | Cr/Au, Cr/Cu, Al
SiO_2 | Si_3N_4, Cr, Cr/Cu/Cr
Ni | NiO_x

Fig. 2. Technological route to manufacture MEMS gas sensor

At the second stage (Fig. 2), the topology of the metallization layer was formed, including heating elements, measuring interdigital electrodes, contact pads and connecting paths. Vacuum DC-magnetron sputtering of pure nickel with a thickness of 100 nm was used to apply the metal coating. Next, the topology was formed on the metal layer using direct photolithography. The type of photomasks used is shown in Fig. 3. Nickel etching was carried out in 30 % nitric acid solution.
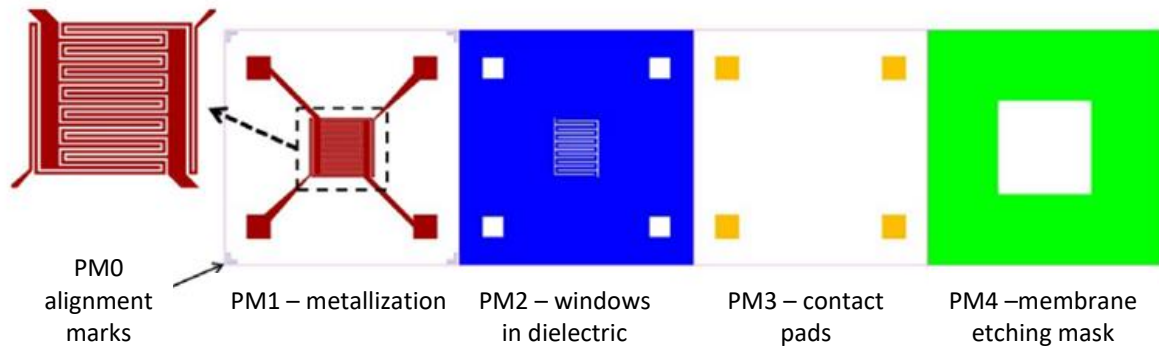
Fig. 3. Topology of used photomasks

To insulate the heater, a SiO_2 dielectric film with a thickness of 300 nm was deposited on the surface of the heating element. This operation was performed using the lift-off photolithography method exposed to PM2 "windows in dielectric" mask. The SiO_2 layer was deposited by vacuum reactive DC-magnetron sputtering of a pure silicon target in an oxygen and argon atmosphere (1:1) at a pressure of 2 mTorr and a discharge power of 150 W at a rate of 2 nm/min. The photoresist was removed in a boiling solution of dimethylformamide and monoethanolamine (1:1), resulting in the formation of contact windows in the deposited dielectric film above the measuring electrodes and microwire bonding pads. To ensure guaranteed heater insulation, the procedure with the application of the insulating layer was performed twice. In addition, to improve the contact pads located at the edges of the chip, a repeated nickel metallization procedure using the lift-off photolithography and vacuum magnetron sputtering of metal.

The penultimate step of the technological route was the etching of the silicon membrane. The topology of the mask was formed using the PM4 "mask for membrane" (Fig. 3). The choice of a specific method of membrane fabrication, as well as modes of silicon etching and chemical reagents used, was made in accordance with the chemical resistance of the elements on the front surface.
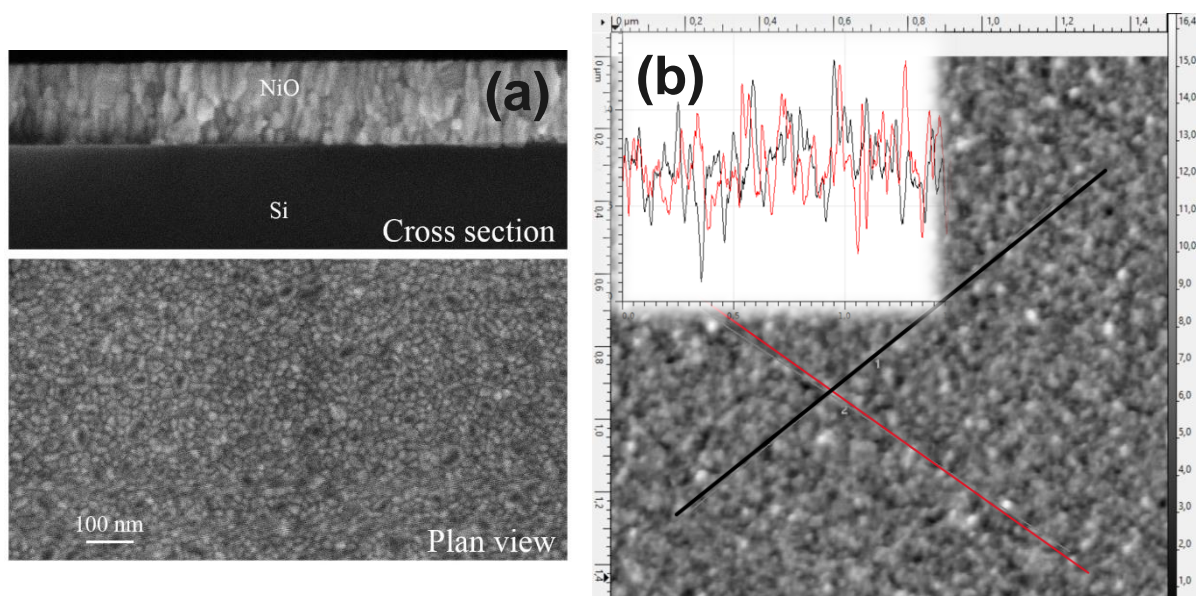
Fig. 4. (a) SEM and (b) AFM images of nickel oxide layer with the thickness of 120 nm

Deposition of the gas-sensitive NiO layer on the central area of the chips was performed through an overlay mask made of a silicon plate with laser-cut square holes (Fig. 2). Vacuum reactive DC-magnetron sputtering of a nickel target with a diameter of 100 mm [21] and a thickness of 1 mm in an atmosphere consisting of 30 % oxygen and 70% argon (O_2 flow rate of 6 sccm, Ar flow rate of 14 sccm) [22] was used for the deposition. The operating pressure during sputtering was 3 mTorr, the discharge power was about 100 W (0.3 A, 340 V), and the distance from the target to the chip substrate holder was 20 cm. The NiO deposition rate was 2 nm/min. The thickness of the deposited coating varied from 30 to 120 nm, and the thin film morphology is shown in Fig. 4 [6,14,15].

To increase the proportion of the crystal phase in the deposited NiO films, annealing was performed at 300–550 °C [23–26]. The annealing temperature was limited to 400 °C, since at higher temperatures significant degradation of the metallization system occurred.

Results and discussion

To study the gas sensitivity of the MEMS SEs, they were placed for mounting in metallized ceramic boards (Fig. 5(a)), which have low thermal conductivity to reduce overall power consumption. The use of such layouts for mounting contacts allowed to protect the metal contacts of SE, as the most vulnerable to the effects of hydrogen sulfide, and to provide flip-chip mounting of SE. The chip in the case is shown in Fig. 5(b).
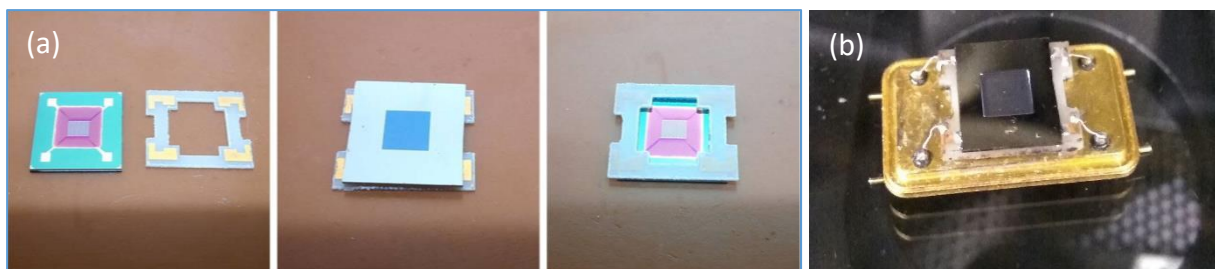

Fig. 5. Polycor boards, MEMS sensor before (a) and after (b) mounting

Measuring the main electrical parameters of the MEMS sensor

Before determining the sensitivity to the presence of hydrogen sulfide of known concentration, the basic electrical parameters of the laboratory MEMS sensor prototypes were measured, such as the resistance of the heater and gas-sensitive layer at different temperatures.

During the measurements, each chip with the MEMS sensor was subjected to slow heating and cooling. During this time, the resistance values of the nickel heater and the NiO sensitive layer between the measuring interdigital electrodes were measured. The chips both with and without annealing were used for the measurements. Figure 6 shows the characteristic temperature dependences of the resistances for five SEs with nickel oxide layer with a thickness of 120 nm, differing in high-temperature annealing modes.

Subsequently, the parameters of the obtained calibration curves allowed estimating the temperature of the sensor's operating zone by extrapolating the obtained dependencies to the entire temperature range.

(a)

(b)

(c)

(d)

(e)
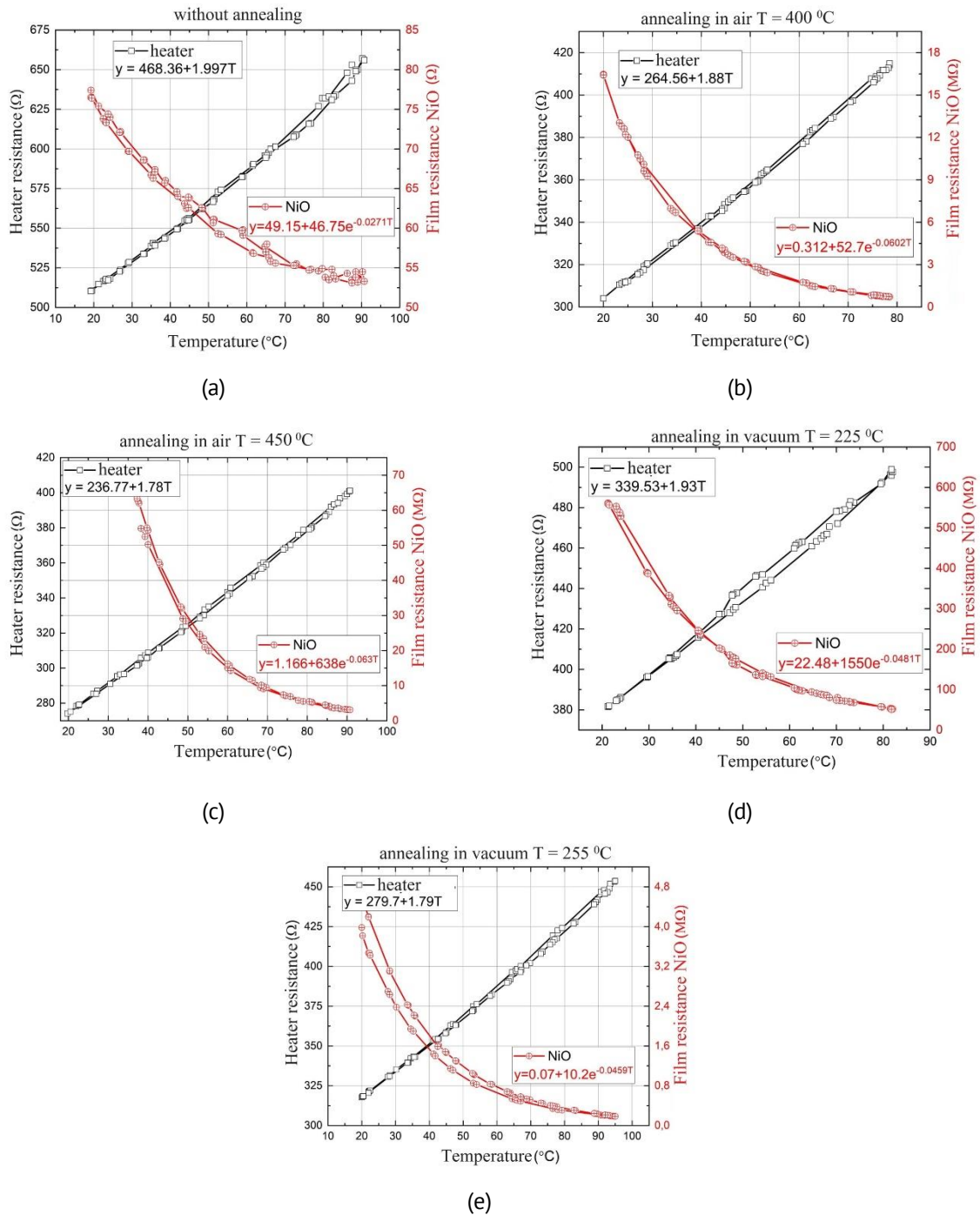
Fig. 6. Temperature dependences of the resistance of the heater and the gas-sensitive layer of NiO without annealing (a), with vacuum annealing (residual pressure 10^{-6} Pa) (b,c) and annealing in air (d,e)

Effect of annealing temperature on the electrical parameters of the active layer

All annealed SE samples are characterized by a linear temperature dependence of the measured resistance (conductivity) in semi-logarithmic coordinates (Fig. 7(b)), which indicates the formation of a high-quality polycrystalline layer of semiconductor NiO and the ohmic nature of the metal contacts burned into it [15,17]. For the SE without annealing, this dependence is nonlinear, which may indicate either an amorphous state of the gas-sensitive layer or poor quality of the contacts [27].

(a)   (b)
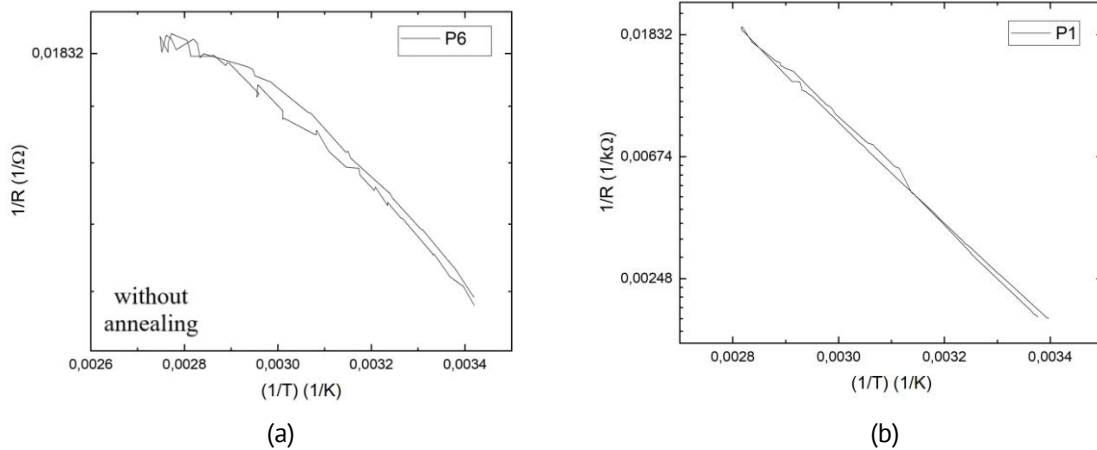
Fig. 7. Temperature dependences of the conductivity of the gas-sensitive layer of the SE in semi-logarithmic coordinates before (a) and after (b) annealing of NiO

The absolute value of the resistance of the nickel heater decreases with increasing annealing temperature in each series of experiments, in the range from 850 to 500 ohms, and its temperature coefficient of resistance is almost constant in the studied temperature range [28].

(a)   (b)

(c)
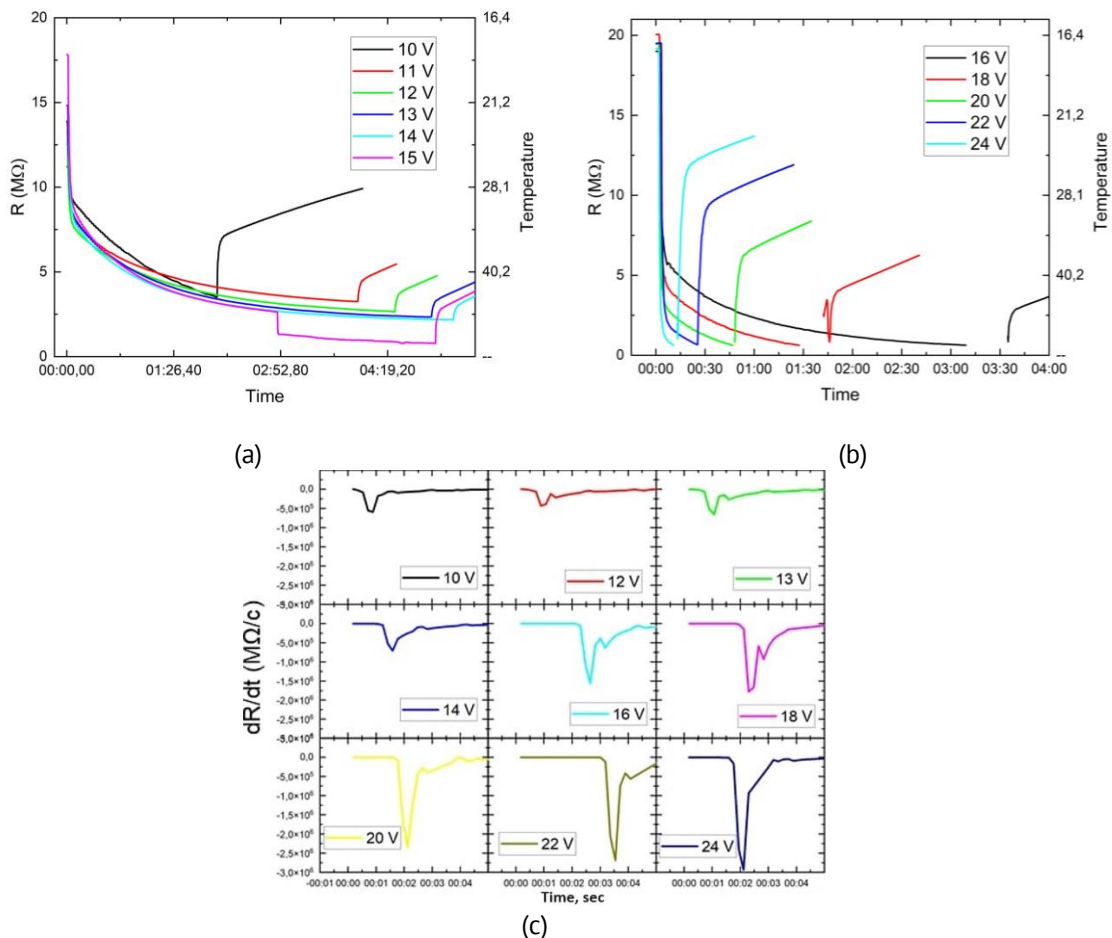
Fig. 8. Change in the resistance of the NiO gas-sensitive layer over time (min) when the heater is switched on and off at different voltages on the heater: (a) heating/cooling time of the sensor when applying voltage to the heater from 10 to 15 V (power < 1 W); (b) heating/cooling time of the sensor when applying voltage to the heater from 16 to 24 V (power > 1 W); (c) derivative of the heater resistance when applying voltage in pulse mode

Sensor response time

Figure 8 shows the experimental time characteristics of one of the laboratory models of the SE at different values of voltage supplied to the heater. These dependencies are characterized by two time intervals both on the heating curve and on the cooling curve – a rapid change [22,29] in the temperature of NiO at the initial moment of the response time (t_{90}) of several seconds and slow thermal stabilization of the SE within several minutes after switching on or off the supply voltage.

## Power consumption parameters for different operating temperatures

The power consumption of the formed SE was from 0.5 to 1.5 W (Fig. 9) in the operating temperature range. During the study, it was found that despite the presence of the membrane, during heating, the sample case is strongly heated. In order to reduce the heating, it was proposed to use additional "legs" for thermal decoupling of the sample. The "legs" were metal pins on the back surface of the case, which were supposed to improve heat dissipation. However, the presence of "legs" did not give the expected results. The reason for this may be the strong influence of convective heating of the case due to the large area of the heater and the small gap in the case.
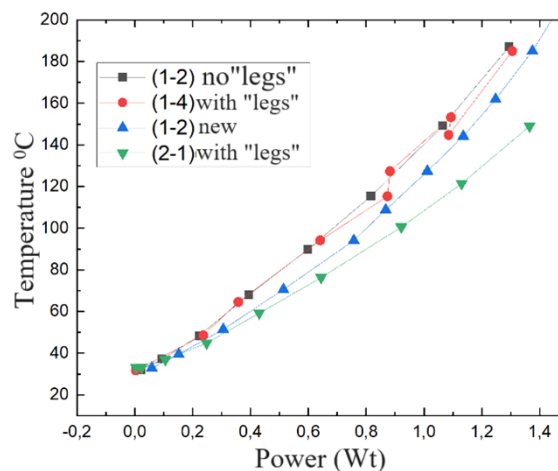
Fig. 9. Experimental dependences of the heater temperature on the power supply for different installation conditions in the case (with and without "legs")

Study of the sensitivity of a gas sensor to hydrogen sulfide

For *p*-type semiconductors, interaction with gases by the reduction mechanism leads to a decrease in resistance, which is caused by an increase in the number of holes in the valence band due to a decrease in the number of electrons as a result of chemical sorption of gas on the surface. The reverse mechanism is observed with the oxidation mechanism. This changes the geometric size of the space charge region and other parameters of the semiconductor film related to its conductivity. This is demonstrated schematically in Fig. 10. In the case of the nickel oxide film, an increase in the resistance of the active layer is expected with increasing temperature when interacting with hydrogen sulfide.
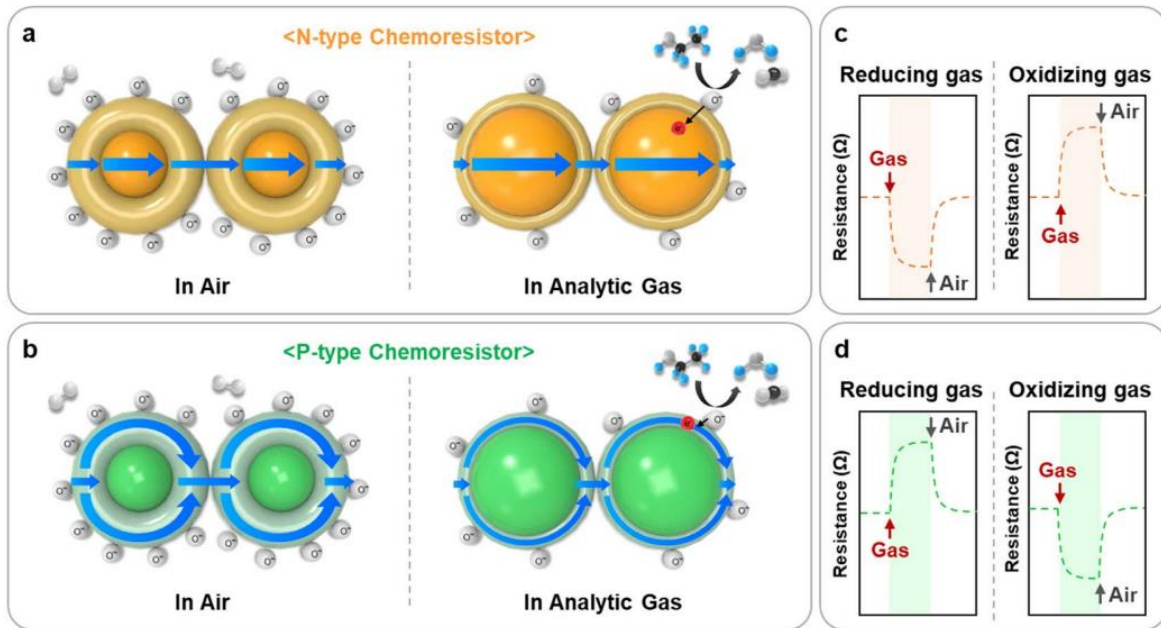
Fig. 10. Gas detection mechanism and transient resistance changes of *n*-type (a,c) and *p*-type (b,d) chemoresistive gas sensors

The tests of the manufactured MEMS sensor elements were carried out using a measuring stand consisting of a chamber, a gas distribution system for hydrogen sulfide (with a maximum hydrogen sulfide concentration in the chamber of 100 ppm), a reference hydrogen sulfide sensor "ATOM MIRAX", and the corresponding electronic equipment for signal recording. Resistance measurements were carried out using a resistive divider circuit [30] based on precise calibration resistances (Fig. 11).
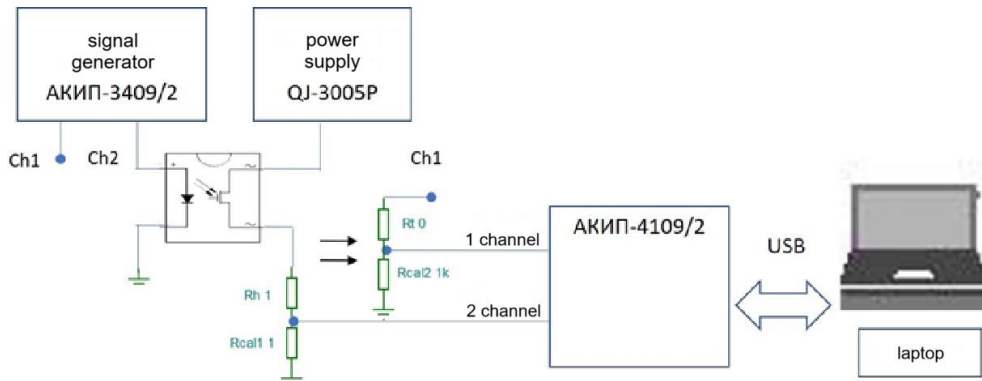

Fig. 11. Scheme of measuring system: R_t is thermistor; R_h is heater, R_{cal} are current measuring resistors

The SE was tested at heater operating temperatures from 130 to 205 °C to exclude the influence of changes in the registered signal from the flow rate. In the measurements, the gas flow rate was maintained constant using two GMFCs; the total flow was 3.6 l/h. Figure 12 shows an example of the dependences of hydrogen sulfide influence on the sensor resistance in comparison with the reference hydrogen sulfide sensor for different gas supply ratios at the operating temperature, and also indicates the heater temperature drift during measurements at 130, 170, 205 °C. The formed SE allowed to detect from 1 to 100 ppm of hydrogen sulfide.
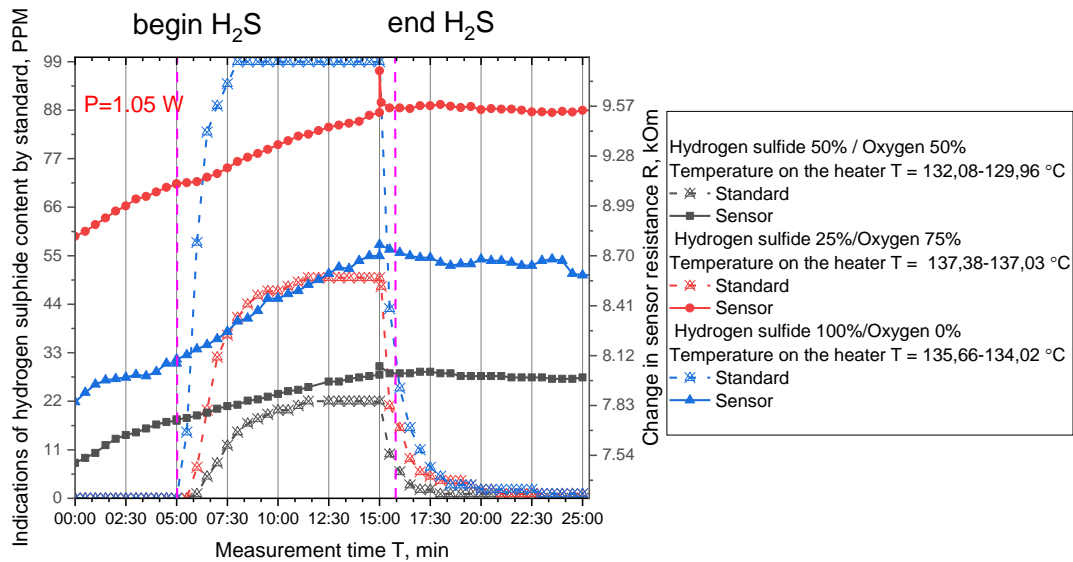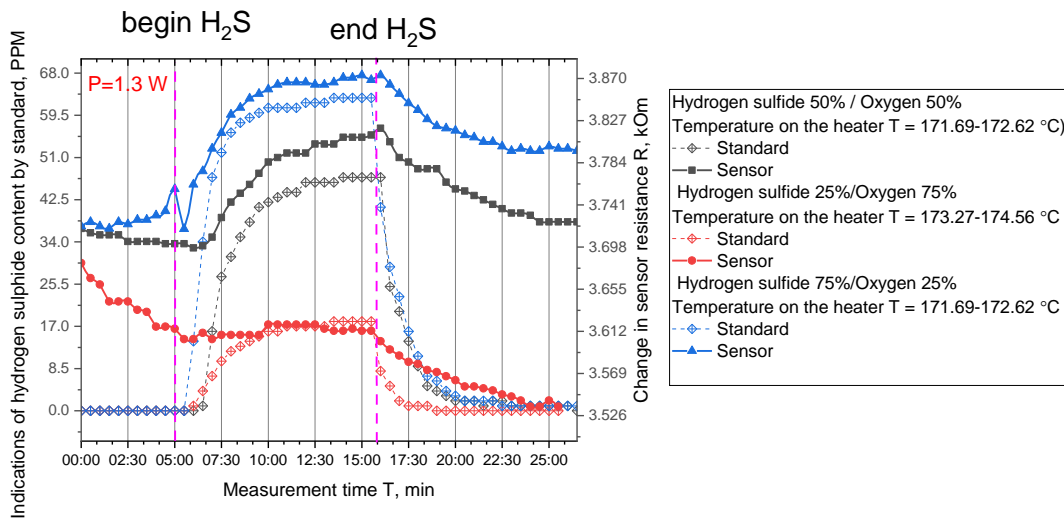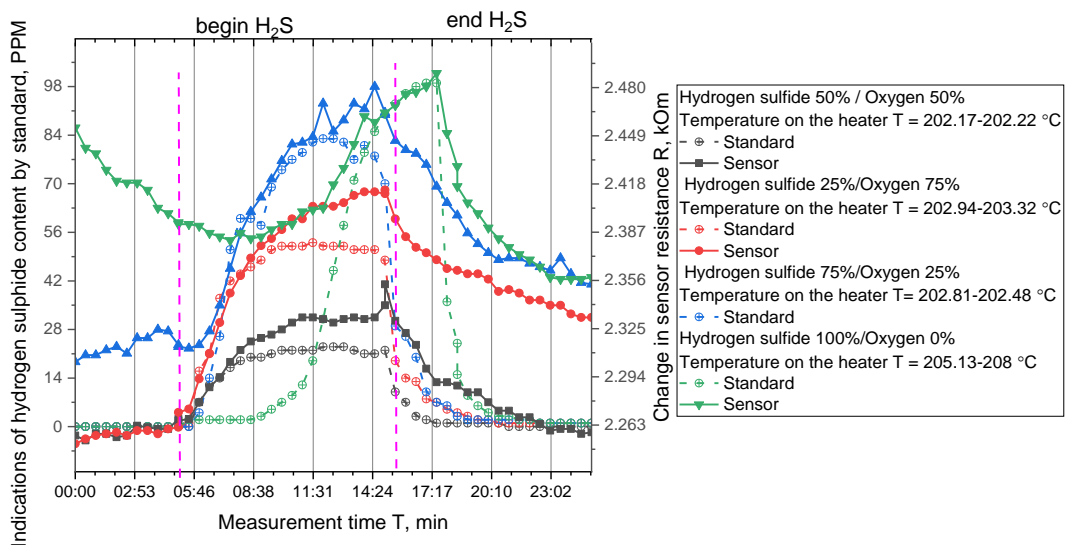
Fig. 12. Dependencies of the influence of hydrogen sulfide on the resistance of the sensor in comparison with the reference sensor for different gas supply ratios (as a percentage of the total volume of gases in the mixture), at different operating temperatures: (a) 130 °C, (b) 170 °C, (c) 205 °C

Figure 12 shows that the nickel oxide-based gas sensor manufactured using the proposed MEMS technology allows detecting hydrogen sulfide in the range from 1 to 100 ppm. The most effective operating temperature for detecting hydrogen sulfide is 205 °C (Table 1). The operating power of the sensor is 1.45 W. Moreover, the built-in microheater provides a simultaneous heating function without the need for any external heating device. However, a systematic study requires consideration of the selectivity of the sensor when gases other than hydrogen sulfide are also present in the air.

Table 1. Sensor parameters at different operating temperatures

Operating temperature of the sensor, °C	Response to hydrogen sulfide, sec	Power, W	Recorded concentrations, ppm
130	–	1.05	–
170	30	1.30	15–100
205	10	1.45	1–100

Conclusion

The article proposes and tests a technology for manufacturing MEMS hydrogen sulfide sensors with a sensitive layer of nickel oxide. The sensitive layer of nickel oxide (NiO) showed sensitivity to hydrogen sulfide from 1 to 100 ppm, for annealed films at a temperature of 300 to 400 °C, the optimal operating temperature was 205 °C. The presence of a silicon membrane made it possible to reduce energy consumption to several watts, due to a decrease in the heat capacity of the chip while maintaining the size and design of the heater. The MEMS sensor showed a thermal stabilization time of about a minute, under the condition of a sharp primary heating of about 1 sec.

This resistive-type MEMS sensor with a self-heating thin NiO film is suitable for energy-efficient gas sensor applications but requires testing for selectivity.

References

1. Dong Y, Gao W, Zhou Q, Zheng Y, You Z. Characterization of the gas sensors based on polymer-coated resonant microcantilevers for the detection of volatile organic compounds. *Analytica Chimica Acta.* 2010;671(1–2): 85–91.
2. Zampolli S, Elmi I, Ahmed F, Passini M, Cardinali GC, Nicoletti S, Dori L. An electronic nose based on solid state sensor arrays for low-cost indoor air quality monitoring applications. *Sensors and Actuators B: Chemical.* 2004;101(1–2): 39–46.
3. Tomchenko AA, Harmer GP, Marquis BT, Allen JW. Semiconducting metal oxide sensor array for the selective detection of combustion gases. *Sensors and Actuators B: Chemical.* 2003;93(1–3): 126–134.
4. He L, Jia Y, Meng F, Li M, Liu J. Development of sensors based on CuO-doped SnO_2 hollow spheres for ppb level H_2S gas sensing. *Journal of Materials Science.* 2009;44(16): 4326–4333.
5. Kanan SM, El-Kadri OM, Abu-Yousef IA, Kanan MC. Semiconducting Metal Oxide Based Sensors for Selective Gas Pollutant Detection. *Sensors.* 2009;9: 8158–8196.
6. Park SJ, Lee SM, Oh MH, Huh YS, Jang HW. Food quality assessment using chemoresistive gas sensors: achievements and future perspectives. *Sustainable Food Technology.* 2024;2: 266–280.
7. Wang C, Yin L, Zhang L, Xiang D, Gao R. Metal Oxide Gas Sensors: Sensitivity and Influencing Factors. *Sensors.* 2010;10(3): 2088.
8. Santhosh S, Balamurugan K, Mathankumar M, Shankar K, Subramanian B. Electrochromic and optical studies on Nb_2O_5–NiO mixed oxide films for smart window applications. *Optical Materials.* 2023;135: 113248.
9. Huang X, Meng F, Pi Z, Xu W, Liu J. Gas sensing behavior of a single tin dioxide sensor under dynamic temperature modulation. *Sensors and Actuators B: Chemical.* 2004;99(2–3): 444–450.

10. Hyodo T, Nishida N, Shimizu Y, Egashira M. Preparation and gas-sensing properties of thermally stable mesoporous SnO_2. *Sensors and Actuators B: Chemical.* 2002;83(1–3): 209–215.

11. Kondrateva AS, Bespalova PG, Filatov LA, Tanklevskaya EM, Pavlov SI, Alexandrov SE. Gas-sensitive properties of thin nickel oxide films. *Russian Journal of Applied Chemistry.* 2017;90(6): 846–852.

12. Chen H, Ma H, Zhu Y, Zhao M, Chen Z, Zhang L. Novel approach for improving electrochromic and mechanical properties of NiO film: Experiment and molecular dynamics simulation. *Applied Surface Science.* 2023;609: 155209.

13. Lee CY, Chiang CM, Wang YH, Ma RH. A self-heating gas sensor with integrated NiO thin-film for formaldehyde detection. *Sensors and Actuators B: Chemical.* 2007;122(2): 503–510.

14. Sun YF, Liu SB, Meng FL, Liu JY, Jin Z, Kong LT, Liu JH. Metal oxide nanostructures and their gas sensing properties: A review. *Sensors.* 2012;12(3): 2610–2631.

15. Lee CY, Hsieh PR, Lin CH, Chou PC, Fu LM, Chiang CM. MEMS-based formaldehyde gas sensor integrated with a micro-hotplate. *Microsystem Technologies.* 2006;12: 893–898.

16. Wang Y, Liu C, Wang Z, Song Z, Zhou X, Han N, Chen Y. Sputtered SnO_2:NiO thin films on self-assembled Au nanoparticle arrays for MEMS compatible NO_2 gas sensors. *Sensors and Actuators B: Chemical.* 2019;278: 28–38.

17. Gatty HK, Stemme G, Roxhed N. A miniaturized amperometric hydrogen sulfide sensor applicable for bad breath monitoring. *Micromachines.* 2018;9(12): 612.

18. Bonaccorsi L, Malara A, Donato A, Donato N, Leonardi SG, Neri G. Effects of UV Irradiation on the Sensing Properties of In_2O_3 for CO Detection at Low Temperature. *Micromachines.* 2019;10(5): 338.

19. Donato N, Grassini S. Editorial for the Special Issue on Nanostructure Based Sensors for Gas Sensing: from Devices to Systems. *Micromachines.* 2019;10(9): 591.

20. Wang F, Jia J, Zhao W, Zhang L, Ma H, Li N, Chen Y. Preparation and electrochromic properties of NiO and ZnO-doped NiO thin films. *Materials Science Semiconductor Processing.* 2022;151: 106986.

21. Tan S, Gao L, Wang W, Gu X, Hou J, Su G. Preparation and black-white electrochromic performance of the non-contact ZnO@NiO core-shell rod array. *Surfaces and Interfaces.* 2022;30: 101889.

22. Zhang L, Zhao M, Chen Y, Chen H, Wang F, Ma L, Ma H. Effect of sputtering pressure on the electrochromic properties of flexible NiO films prepared by magnetron sputtering. *Materials Letters.* 2024;354: 135317.

23. Tuna Ö, Mak AK, Öztürk O, Karabulut M. Influence of oxygen partial pressure on the structural, optical and electrochromic properties of NiO thin films grown by magnetron sputtering. *Applied Physics A.* 2023;129(12): 820.

24. Choi D, Son M, Im T, Ahn SH, Lee CS. Microstructure control of NiO-based ion storage layer with various sized NiO particles to evaluate the electrochromic performance. *Materials Chemistry and Physics.* 2020;249: 123121.

25. Li Z, Yu Z, Wang W, Hou J, Gao L, Gu X, Su G. Nickel oxide film with tertiary hierarchical porous structure and high electrochromic performance and stability. *Materials Chemistry Physics.* 2021;269: 124738.

26. Ivanova T, Harizanova A, Koutzarova T, Vertruyen B. Preparation and Investigation of Sol–Gel TiO_2-NiO Films: Structural, Optical and Electrochromic Properties. *Crystals.* 2024;14(2): 192.

27. Goel R, Jha R, Ravikant C. Nickel oxide (NiO) nano-triangles with enhanced electrochromic and photovoltaics properties. *Chemical Papers.* 2023;77(5): 2885–2903.

28. Wruck DA, Rubin M. Structure and Electronic Properties of Electrochromic NiO Films. *Journal of the Electrochemical Society.* 1993;140: 1097.

29. Jia J, Chen Y, Zhang W, Wang Z, Wang F, Zhang L, Ma H. Experimental study and simulation of electrochromic properties of TiO_2-doped NiO films. *Ceramics International.* 2024;50(9): 15065–15075.

30. Niu G, Zhuang Y, Hu Y, Liu Z, Wang F. Selective Discrimination of Ppb-level Vocs Using Mos Gas Sensor in Pulse-Heating Mode with the Modified Hill's Model. In: *Proceedings of the IEEE International Conference on Micro Electro Mechanical Systems (MEMS).* Institute of Electrical and Electronics Engineers Inc.; 2023: 826–829.

About the Authors

Ivan M. Komarevtsev ⓘD Sc

Researcher (Alferov University, St. Petersburg, Russia)

Anastasia S. Kondrateva ⓘD Sc

Candidate of Chemical Sciences
Associate Professor (Alferov University, St. Petersburg, Russia)

Alexei N. Kazakin iD Sc
Engineer (Alferov University, St. Petersburg, Russia)

Yakov B. Enns iD Sc
Researcher (Alferov University, St. Petersburg, Russia)

Ilya A. Lazdin iD Sc
Engineer (Peter the Great St. Petersburg Polytechnic University, St. Petersburg, Russia)

Platon A. Karaseov iD Sc
Doctor of Physical and Mathematical Sciences
Professor (Peter the Great St. Petersburg Polytechnic University, St. Petersburg, Russia)

Yurie D. Akulshin iD Sc
Lead Engineer (Peter the Great St. Petersburg Polytechnic University, St. Petersburg, Russia)